DYNAMIC-LUMPED PARAMETER MODEL OF A HEAT PUMP - SENSITIVITY ANALYSIS FOR PERFORMANCE OPTIMIZATION

R. Lepore, Senior Researcher, Energy Research Centre, Mons University, Belgium
M. Remy, Professor, Control Department, Mons University, Belgium
E. Dumont, Assistant, Thermodynamics Department, Mons University, Belgium
M. Frère, Professor, Thermodynamics Department, Mons University, Belgium

Abstract: A heat pump dedicated to building heating must exhibit sufficient efficiency (usually measured by the coefficient of performance) in order to comply with low energy consumption and CO_2 production. Good performance can be achieved through capacity control. In this study, the authors evaluate the impact of the capacity adjustments on the transient behaviour of the heat pump. A dynamic, lumped-parameter model is used, which is composed of moving-boundary exchanger sub-models, static compressor and expansion valve sub-models. It is shown, by examining the transfer function of the expansion valve-superheating system, that changes in the compressor flow rates may influence seriously the control of the superheating. Future developments should be devoted to further investigation with respect to capacity control but also to model refinement and validation through experience.

Key Words: heat pump, dynamic modelling, control design

1 INTRODUCTION

In temperate European countries, air-to-water heat pumps appear more and more convenient for the heating of residential buildings. They extract energy from the ambiance and they deliver it, for example, to a piped heating floor for low-temperature heating. A heat pump based on vapour compression must exhibit a sufficient *coefficient of performance (COP)* in order to compete with traditional gas boilers with respect to fossil energy consumption and CO_2 emission. The COP indicator depends essentially on the cold source and hot sink temperatures, which are globally set by the outside conditions and by comfort requirements. However, the design of the heating system may also impact negatively on the heat pump performance as traditional sizing results in oversized heat pumps, thus in shorter heating duty cycles operating at higher floor and circulating-water temperatures. Controlling the heat pump capacity appears as a major feature in order to deliver heat by using longer duty cycles at lower hot sink temperatures, which enhances the COP (Karlsson 2007). The studies demonstrating these important results are usually based on algebraic energy models, which describe the heat pump at steady state.

This study evaluates the impact of capacity modification on the transient behaviour of the heat pump by using a dynamic model. The dynamic modelling of vapour compression refrigerating systems has been addressed for many years, as described by (Bendapudi and Braun 2002) in their review. More recently dynamic models of moderate complexity (based on moving-boundary sub-models of the exchangers) have been adopted in order to develop control strategies (Rasmussen 2002, Rasmussen 2005, Schurt 2009). Interesting aspects of control design, which pertain to the selection of controlled and control variables, have also been investigated in (Jensen et al. 2007a) and (Jensen et al. 2007b).

The dynamic model used in this work has been introduced in a previous study (Lepore et al. 2010). It is based on a lumped-parameter, moving-boundary sub-model of the heat

exchangers (Willatzen et al. 1998, Rasmussen 2002) whereas the compressor and expansion valve sub-models are static ones. As illustrated in (Lepore et al. 2010), the model represents sufficiently the major dynamics of the heat pump to investigate its behaviour when changes occur in sizing or are due to perturbations (outdoor temperature). Here we investigate the effect of changes due to higher-level control actions on the capacity of the heat pump. In particular, the behaviour of the superheating control is analyzed. In the first experiment, it is assumed that the control action is restricted to the compressor speed, so that simulations are performed for several swept flow rates. In the second experiment, it is assumed that the secondary fluid pumps can also be manipulated so that all the flow rates are changed proportionally.
The rest of the article is as follows. Section 2 presents the complete model of the heat pump from the theoretical and implementation viewpoints. Section 3 introduces the simulation results obtained when modifying the compressor/secondary fluid flow rates. Conclusions are found in Section 4.

2 HEAT PUMP MODEL

Figure 1 represents the heat pump scheme (Figure 1a) and the corresponding thermodynamic cycle of the refrigerant (Figure 1b):

- Heat is extracted from the cold source by successive evaporation (7-1) and superheating (1-2) of the refrigerant at low pressure p_{ev}; the evaporator is a counter-current exchanger with a glycol-water mix as a secondary fluid;
- The refrigerant is compressed adiabatically (2-3) from low pressure p_{ev} to high pressure p_{co};
- Heat is delivered to the hot sink by successive de-superheating (3-4), condensation (4-5) and subcooling (5-6) of the refrigerant at high pressure p_{co}; the condenser is a counter-current exchanger with water as a secondary fluid;
- The refrigerant is subject to an isenthalpic expansion (6-7) from high pressure p_{co} to low pressure p_{ev}.

In the sequel, the refrigerant transformations in the exchangers are described. In the next step, we present the static models of the compressor and of the expansion valve. Finally, the energy fluxes transmitted in the exchangers from or to the secondary fluids are added to make up the total model.

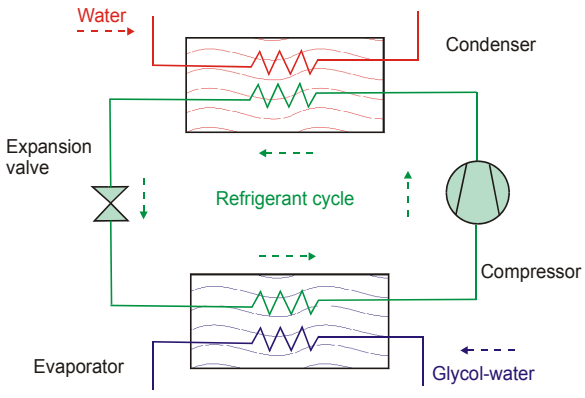


Figure 1a: Heat pump scheme

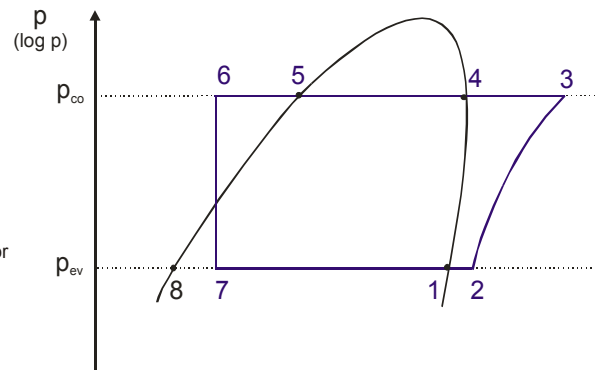


Figure 1b: Heat pump cycle

2.1 Dynamic modelling of the exchangers

2.1.1 Model of a single refrigerant transformation

Figure 2 represents schematically a fraction of an exchanger duct with cross-section *S* and with moving boundaries *a(t)* and *b(t)*, in which the refrigerant is subject to a single transformation. The fluid enters at *a(t)* with mass flow rate q_i and enthalpy h_i, and exits at *b(t)* with mass flow rate q_o and enthalpy h_o. A heat flow rate of density $\Phi(t)$ (in W/m^2) is transmitted through the external surface area of the duct. As described in Rasmussen (2002) and the references therein, it is assumed that the refrigerant has uniform properties all over a cross-section and is not subject to pressure drop.

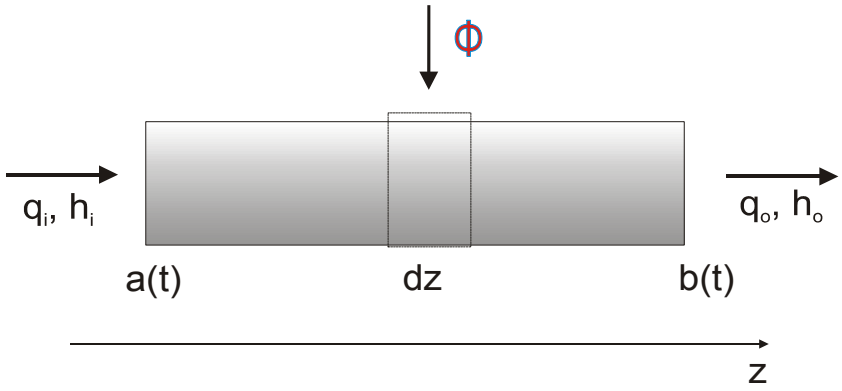


Figure 2: Moving-boundary exchanger part with single refrigerant transformation

The application of mass and thermodynamic balances to the elementary volume *dV=S.dz* leads to two partial differential equations summarized in (1), in which *ρ* is the fluid density, *q* is the mass flow rate whereas *η* and *E* are symbolic values.

$$\frac{\partial(\rho\eta)}{\partial t} + \left(\frac{1}{S}\right)\frac{\partial(q\eta)}{\partial z} = \mathrm{E} \qquad (1)$$

To make it clear,

- if *η* and *E* are set to *1* and *0,* respectively, equation (1) expresses the mass balance;
- if *η* and *E* are set to *h* and $\partial p/\partial t + F\phi$, respectively, equation (1) expresses the energy balance; in this case, *h* is the enthalpy, *p* is the pressure, ϕ is as above and *F* is a shape factor, equal to the ratio of the cross-section perimeter to the cross-section area *S*.

Equation (1) can be integrated spatially by using the integration rule of Leibniz where the integration boundaries are time-varying. This yields time differential equation (2),

$$(b-a)\frac{d\overline{\rho\eta}}{dt} + (\overline{\rho\eta} - (\rho\eta)_b)\frac{db}{dt} - (\overline{\rho\eta} - (\rho\eta)_a)\frac{da}{dt} + \frac{(q\eta)_a - (q\eta)_b}{S} = \bar{E}(b-a) \qquad (2)$$

where

- *η* and *E* are as described above;
- $\overline{\rho\eta}$ and $\bar{E}$ are the average values of *(ρη)* and *E*, respectively, between *a(t)* and *b(t)* at time *t*, $(\rho\eta)_a$ and $(\rho\eta)_b$ are the corresponding values at the boundaries;

- $q_a \equiv q_i$ and $q_b \equiv q_o$ are the input and output mass flow rates, respectively.

2.1.2 Evaporator model

Figure 3 represents schematically the evaporator from the refrigerant viewpoint, i.e., two duct regions separated by a moving frontier, the first from *0* to $\lambda_{ev}(t)$ corresponds to evaporation (two-phase region), the second from $\lambda_{ev}(t)$ to *L* corresponds to superheating (one-phase region).

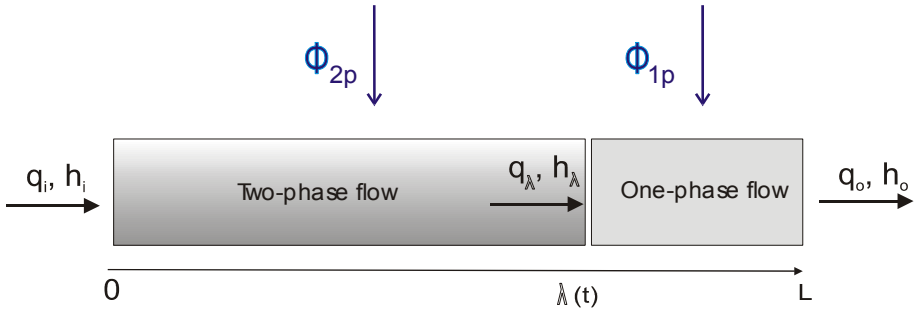


Figure 3: Schematic view of the evaporator

Equation (2) is applied to each zone. For the evaporation zone, $a(t) \equiv 0$ and $b(t) = \lambda_{ev}(t)$ and the average value $\overline{\rho\eta}$ is expressed based on the *mean void fraction* assumption (Wedekind et al., 1978), which states that the vapour and liquid masses occupy fixed volume fractions γ and $(1-\gamma)$, respectively (a typical value of γ is 0.8). Therefore $\overline{\rho\eta}$ can be expanded as

$$\overline{\rho\eta} = \gamma(\rho_v\eta_v) + (1-\gamma)(\rho_l\eta_l) \tag{3}$$

Subscripts *v* and *l* refer to *saturated vapour* and *saturated liquid*, respectively. One can note that, in the evaporation zone, $\overline{\rho\eta}$ is a function of one thermodynamic variable, here pressure p_{ev}.
For the superheating zone, $a(t) = \lambda_{ev}(t)$ and $b(t) \equiv L$. Here the average value $\overline{\rho\eta}$ is reasonably approximated by an arithmetic mean as

$$\overline{\rho\eta} = \frac{(\rho_v\eta_v)+(\rho_o\eta_o)}{2} \tag{4}$$

Subscript *o* refers to *outlet*. $\overline{\rho\eta}$ is a function of two thermodynamic variables, here pressure p_{ev} and enthalpy h_o.

As two equations (mass and energy balance) apply for each of the two zones but constrained by a mass conservation condition between the zones, in fact three independent differential equations describe the mass and energy balances of the evaporator. On the other hand, the expressions of $\overline{\rho\eta}$ for the evaporation zone make it appear the time derivatives of ρ_l, ρ_v, $(\rho_l h_l)$ and $(\rho_v h_v)$, which leads, for example in the case of $(\rho_l h_l)$, to

$$\frac{d(\rho_l h_l)}{dt} = \left(\frac{d\rho_l}{dp} + \frac{dh_l}{dp}\right)\frac{dp_{ev}}{dt} \equiv \left(\rho_l' + h_l'\right)p_{ev}'(t) \tag{5}$$

For the superheating zone, the time derivatives of ρ_o and $(\rho_o h_o)$ lead, for example in the case of ρ_o, to

$$\frac{d\rho_o}{dt} = \frac{d\rho_o}{dp}\frac{dp_{ev}}{dt} + \frac{d\rho_o}{dh}\frac{dh_o}{dt} \equiv \rho_o' p_{ev}'(t) + \rho_o^* h_o'(t) \tag{6}$$

Note that, conventionally, superscripts ‘ and *, when applied to any thermodynamic variable but pressure or enthalpy, will denote its partial derivative with respect to pressure and enthalpy, respectively. Superscript ‘, when applied to pressure or enthalpy, will denote the time derivative.

Finally the differential equations for the evaporator read as follows

$$G_{ev}(\vec{x}_{ev})\vec{x}'_{ev} = \vec{f}_{ev}(\vec{x}_{ev}, \vec{u}_{ev})$$

$$\vec{x}_{ev} = [\, p_{ev} \quad \lambda_{ev} \quad h_{o;ev} \,]^T$$

$$\vec{f}_{ev}(\vec{x}_{ev}, \vec{u}_{ev}) = \frac{1}{S_{ev}} \begin{bmatrix} (q_{i;ev} - q_{o;ev}) \\ q_{i;ev}(h_{i;ev} - h_{v;ev}) + \Phi_{ev;2p} \\ q_{o;ev}(h_{v;ev} - h_{o;ev}) + \Phi_{ev;1p} \end{bmatrix} \tag{7}$$

$G_{ev}(.)$ is a *3×3* non-singular matrix whose description is found in (Lepore et al. 2010), $\vec{u}_{ev}$ is the external input vector. $\Phi_{ev;2p}$ and $\Phi_{ev;1p}$ are the heat flow rates (in W) transmitted to the evaporation and superheating zones, respectively.

2.1.3 Condenser model

The same model as the evaporator one is adopted for the condenser (i.e., a two-phase zone followed by a one-phase zone) thanks to the assumption that the de-superheating phase is embedded into the condensation phase. This assumption is reasonable given the lower energy amount involved in the de-superheating compared to the condensation one. However, considering the de-superheating phase individually is a priority for future developments. This way the condenser is viewed as two zones with a moving frontier at $\lambda_{co}(t)$: the condensation zone, from *0* to $\lambda_{co}(t)$, and the subcooling zone, from $\lambda_{co}(t)$ to *L*. Expressing the average value $\overline{\rho\eta}$ lies on similar assumptions as for the evaporator , i.e, in the condensation region, the vapour and liquid phases occupy constant volume fractions *γ* and *(1- γ)*, whereas in the subcooling region, the average value $\overline{\rho\eta}$ is just an arithmetic mean of the corresponding saturated liquid and output values (note that this assumption for the liquid phase of the condenser is even less drastic than for the vapour phase of the evaporator).

Finally the differential equations for the condenser read as follows

$$G_{co}(\vec{x}_{co})\vec{x}_{co}{}' = \vec{f}_{co}(\vec{x}_{co}, \vec{u}_{co})$$

$$\vec{x}_{co} = [\, p_{co} \quad \lambda_{co} \quad h_{o;co} \,]^T$$

$$\vec{f}_{co}(\vec{x}_{co}, \vec{u}_{co}) = \frac{1}{S_{co}} \begin{bmatrix} (q_{i;co} - q_{o;co}) \\ q_{i;co}(h_{i;co} - h_{v;co}) + \Phi_{co;2p} \\ q_{o;co}(h_{v;co} - h_{o;co}) + \Phi_{co;1p} \end{bmatrix} \tag{8}$$

$G_{co}(.)$ is a *3×3* non-singular matrix whose description is found in (Lepore et al. 2010), $\vec{u}_{co}$ is the external input vector. $\Phi_{co;2p}$ and $\Phi_{co;1p}$ are the heat flow rates (in W) transmitted to the condensation and subcooling zones, respectively.

2.2 Static equations of the compressor and of the expansion valve

2.2.1 Compressor equation

A classical model for a reciprocating compressor is adopted. The mass flow rate writes

$$q_{o;ev} = q_{i;co} = q_V \rho_{o;ev}(1 - \epsilon_V[(\frac{p_{co}}{p_{ev}})^{\frac{1}{k}} - 1]) \quad (9)$$

where q_V is the volume swept by the piston per unit of time, ε_V is the dead volume ratio, $k = c_{P;o;ev}/c_{V;o;ev}$, $c_{P;o;ev}$ and $c_{V;o;ev}$ are the specific heats at constant pressure and volume, respectively.

The thermodynamic transformation is calculated using the *isentropic compressor efficiency* $\eta_{iso\text{-}s}$, defined as

$$\eta_{iso-s} = \frac{h_{i;co;iso-s} - h_{o;ev}}{h_{i;co} - h_{o;ev}} \quad (10)$$

where $h_{i;co}$ is the enthalpy at the real point at pressure p_{co}, $h_{i;co;iso\text{-}s}$ is the enthalpy at pressure p_{co} when the compression is isentropic.

2.2.2 Expansion valve equation

The mass flow rate is defined as

$$q_{o;co} = q_{i;ev} = C_d A_v \alpha_v \sqrt{2\, \rho_{o;co}\, (p_{co} - p_{ev})} \quad (11)$$

where C_d is the *valve discharge coefficient*, A_v is the maximum flow section; α_v is a non-dimensional coefficient so that (A_v. α_v) is the effective flow section ($0 \leq \alpha_v \leq 1$).

The thermodynamic transformation is isenthalpic, that is,

$$h_{i;ev} = h_{o;co} \quad (12)$$

2.3 Counter-current exchangers with secondary fluids

In this study, both the evaporator and the condenser are counter-current exchangers assumed with negligible thermal capacity, so that the following heat transfer equation applies

$$\Phi = UA.\frac{(t_{1i} - t_{2o}) - (t_{1o} - t_{2i})}{ln\frac{(t_{1i} - t_{2o})}{(t_{1o} - t_{2i})}} \quad (13)$$

where Φ is the heat flow rate exchanged, UA is the global transfer coefficient (e.g., *in W/K*), t_{1i} and t_{1o} are the input and output temperatures of fluid *1*, t_{2i} and t_{2o} are the input and output temperatures of fluid *2*.

We consider the evaporator, with global transfer coefficient UA_{ev} for the total length L_{ev}, a glycol-water mix as a secondary fluid, constant mass flow rate q_G, constant specific heat $c_{P;G}$ and constant inlet temperature $t_{G;i}$. The heat flow rate exchanged in the superheating region is expressed as follows

$$\Phi_{ev;1p} = UA_{ev}\frac{(L_{ev} - \lambda_{ev})}{L_{ev}}\frac{(t_{Gi} - t_{o;ev}) - (t_{G\lambda} - t_{evap})}{ln\frac{(t_{Gi} - t_{o;ev})}{(t_{G\lambda} - t_{evap})}} = q_G c_{P;G}(t_{Gi} - t_{G\lambda}) \quad (14)$$

Similarly the heat flow rate exchanged in the evaporation region is

$$\Phi_{ev;2p} = UA_{ev}\frac{\lambda_{ev}}{L_{ev}}\frac{(t_{G\lambda}-t_{Go})}{ln\frac{(t_{G\lambda}-t_{evap})}{(t_{Go}-t_{evap})}} = q_G c_{P;G}(t_{G\lambda}-t_{Go}) \quad (15)$$

Similar equations are written for the condenser, with global transfer coefficient UA_{co} for the total length L_{co}, water as a secondary fluid, constant mass flow rate q_W, constant specific heat $c_{P;W}$ and constant inlet temperature $t_{W;i}$.

Relations (13-15) are given here for the sake of comprehension, however the exchanger equation forms using exchanger efficiencies have been used, which allowed to solve explicitly the algebraic equations of the total system.

2.4 Total equation system

Sections (2.1-2.4) have explained the equations of the subsystems making the heat pump. Their detailed description and how they are assembled are beyond the scope of this article. However let us note that the algebraic equations could be explicitly solved, so that the total equation system is composed of differential equations only. A summarized expression of the total system is

$$G(\vec{x})\vec{x}' = \vec{f}(\vec{x},\vec{u};\vec{\theta})$$
$$\vec{x} = [\, p_{ev} \quad \lambda_{ev} \quad h_{o;ev}\, p_{co} \quad \lambda_{co} \quad h_{o;co}\,]^T$$

G(.) is a *6×6* block-diagonal non-singular matrix. Usually $\vec{\theta}$ denotes fixed parameters and constants and $\vec{u}$ denotes manipulated/perturbation inputs. But depending on the problem to solve, a parameter can become an input and vice-versa. In this study, for example, the input vector $\vec{u} = [t_{G;i} \quad t_{W;i} \quad \alpha_v]^T$.

2.5 Model implementation and utilization

2.5.1 Dynamic mode

Equations (16) have been implemented using the Matlab® software. As matrix *G(.)* is non-singular, thus invertible, standard solvers for ordinary differential equations (ODEs) are used; the ODE45 solver is elected here. The thermodynamic properties are calculated using the REFPROP® 8.0 software from NIST. The derivatives of the thermodynamic variables with respect to pressure or enthalpy are approximated by a finite-difference method.

2.5.2 Steady-state mode

From equation (16) we derive that, for a heat pump characterized by parameter $\vec{\theta}$ (including the total refrigerant mass) and subject to a given input $\vec{u}_0$, the steady-state variables, noted $\vec{x}_{ss}$, can be computed by solving

$$0 = \vec{f}(\vec{x}_{ss},\vec{u}_0;\vec{\theta}) \quad (17)$$

for $\vec{x}_{ss}$. In fact equations (17) consist of five independent equations as the two mass balance equations are redundant, however variables λ_{ev} and λ_{co} can be computed from each other and the total refrigerant mass. Thus $\vec{x}_{ss}$ consists of exactly five unknowns and the problem is well-conditioned. Additionally problem (17) can be augmented by adding one or both relations (18).

$$0 = t_{o;ev} - t_{evap} - \Delta t^{superh}$$
$$0 = t_{cond} - t_{o;co} - \Delta t^{subcool} \quad (18)$$

When adding the constraint on the superheating, one solves additionally for the steady-state flow section coefficient, $\alpha_{v;ss}$. If, moreover, the constraint on the subcooling is added, the total refrigerant mass can also be determined. These problems are solved numerically by using the Optimization Toolbox of Matlab®, here the FSOLVE function.

2.5.3 Technical data

In recent years a static energy balance model has been validated successfully using the heat pump of a single-family dwelling in Leuze (Namur), Belgium (Dumont et al. 2008). The parameters of the dynamic model have been derived in (Lepore et al. 2010) either from that static model (energy-related parameters) or from the physical characteristics (mass-related parameters of the exchangers). The model parameters are listed in Table 1.

Table 1: Heat pump parameters

Parameter	Value	Units
Evaporator		
UA_{ev}	1200	W/K
S_{ev}	$3.2\ 10^{-3}$	m^2
L_{ev}	0.415	m
q_G	0.36	kg/s
$c_{P;G}$	3340	J/(kg.K)
Condenser		
UA_{co}	800	W/K
S_{co}	$2.4\ 10^{-3}$	m^2
L_{co}	0.461	m
q_W	0.27	kg/s
$c_{P;W}$	4186	J/(kg.K)
Compressor		
q_V	$1.87\ 10^{-3}$	m^3/s
ε_V	0.0434	-
η_{iso-s}	0.58	-
Expansion valve		
(C_dA_v)	$1.05\ 10^{-6}$	m^2
Refrigerant	R404A	

3 RESULTS

Let us consider a heat pump extracting heat from the ambiance through an atmospheric exchanger and delivering it to a house through a heating floor. If the outdoor temperature is 0°C and an indoor temperature of 23 °C is desired, previous studies have shown that typical inlet temperatures of the secondary fluids $t_{G;i}$ and $t_{W;i}$ are -7 °C and 30 °C, respectively. These values are adopted as realistic inputs for our simulation experiments. The superheating is set to 3°C. The subcooling is set to 6°C at nominal conditions (when the refrigerant and secondary fluid flow rates are nominal). Solving the static, augmented optimization problem leads to the steady-state values shown in Table 2. Two simulation experiments are presented hereafter.

Table 2: Steady-state values

Variables	Nominal	Units
p_{ev}	$4.00\ 10^5$	Pa
p_{co}	$17.9\ 10^5$	Pa
λ_{ev}	0.405	m
h_{ev}	$3.65\ 10^5$	J/kg
h_{co}	$2.48\ 10^5$	J/kg
α_v	0.588	-
M_{refr}	0.667	kg
λ_{co}	0.430	m

3.1 Variation in the compressor flow rate

The swept flow rate of the compressor is decreased by 0.1 until 0.4 times its nominal value. In Figure 4 we have represented the steady-state values of some indicators calculated for every compressor flow rate when the 3°C-superheating and the nominal mass are considered. It is noted that:

- pressures p_{ev} and p_{co} vary inversely, whereas the output enthalpies of the exchangers, $h_{o;e}$ and $h_{o;c}$, do not change so much;
- the lengths of the two-phase regions, λ_{ev} and λ_{co}, decrease drastically when the flow rate ratio is less than 0.6;
- the flow section coefficient of the expansion valve α_v decreases steadily, as expected from equation (11) since the pressure difference decreases slowly.

These changes are non-negligible and one can expect that the dynamic behaviour of the heat pump will also be affected. The transfer function between the flow section coefficient and the superheating is evaluated by the response of the superheating to a step in the flow section coefficient (-2% of the steady-state value). Figure 5 represents the responses for different compressor flow rates. More exactly the values shown are the deviations from 3°C divided by the absolute value of the step (thus we obtain a unit step response and comparison is allowed). The rise time of the response grows higher as the compressor flow rate decreases, however until the ratio is 0.5. For a lower ratio (see 0.4), the trends are inverted. Moreover, for a very low ratio (0.2), the zoomed response in Figure 6 exhibits a particular evolution in the early time instants. This response at low compressor flow rates is typical of a non-minimum phase system, which means that careful investigation must be performed for further design of the superheating control.

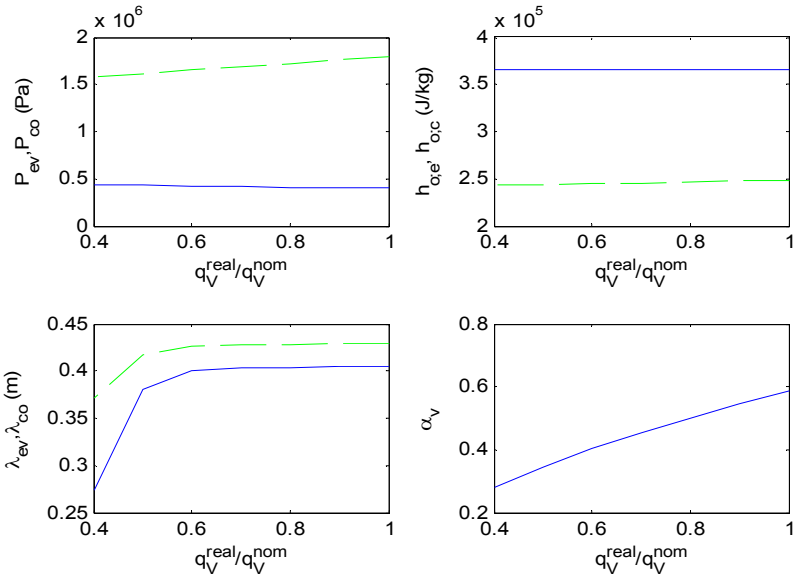


Figure 4: Evolution of the steady state with compression flow rate

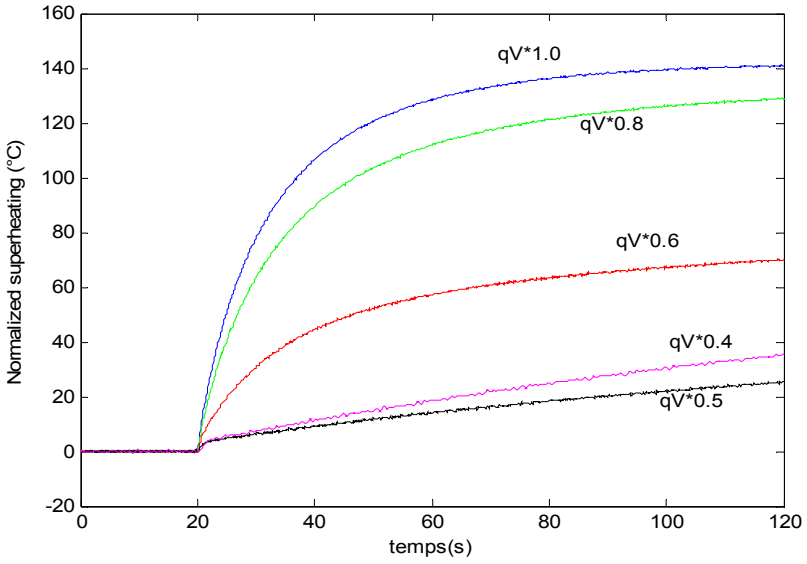


Figure 5: Evolution of the superheating step response with compression flow rate

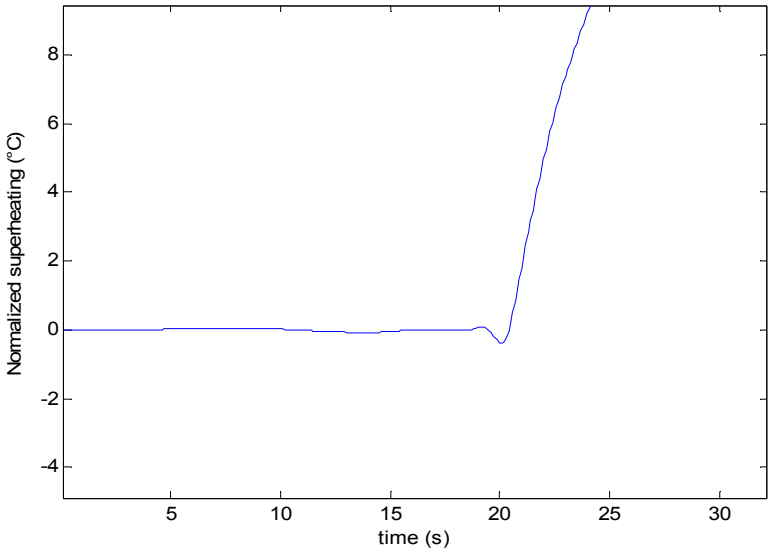


Figure 6: Evolution of the superheating step response at low compression flow rate (ratio is 0.2)

3.2 Variation in the flow rate of the compressor and of the secondary fluids

The swept flow rate of the compressor and the flow rates of the two secondary fluids are simultaneously decreased to 0.8 and 0.6 times their nominal value. In Figure 7 we have represented the responses of the superheating to a step in the flow section coefficient (as described above) for different flow rates. The rise time of the responses is of the same order of magnitude, whatever the flow rates, only a slightly different gain is noted. These differences are due to the fact that the refrigerant mass and the heat transmission coefficients of the exchangers are not adapted.

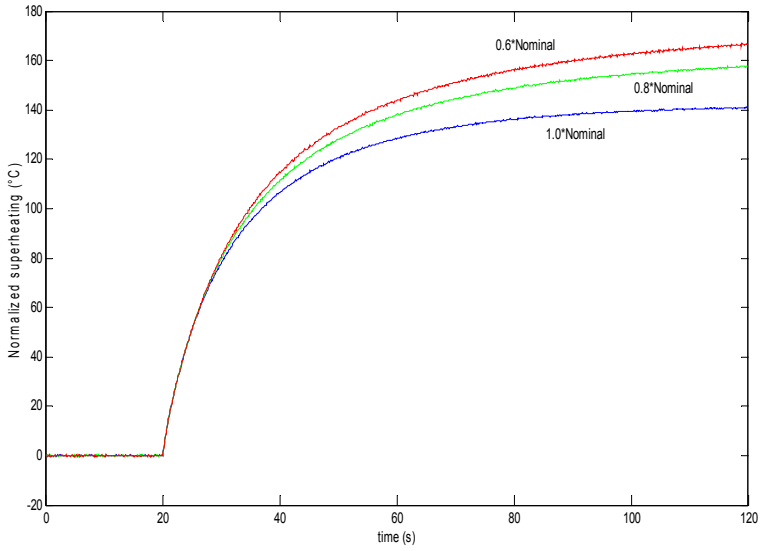


Figure 7: Evolution of the superheating step response with the variation of all flow rates

4 CONCLUSION

Based on our dynamic, lumped-parameter model, we illustrate the effects of capacity control on the dynamic behaviour of the heat pump. Of great interest is the response of the superheating to the effective flow section of the expansion valve. When only the compressor flow rate is decreased, not only the gain decreases but also the speed of the response is affected, which must be carefully considered for further design of the superheating control. Moreover, at low compressor flow rates, a shape modification of the response is noted in the early time instants. When all the flow rates are changed proportionally, the response is much less affected.
Future works should be devoted on the one hand to further investigation on the effects of capacity control, for example when the heat pump is connected to a real load, on the other hand to model validation through experiments.

5 REFERENCES

Bendapudi S., Braun, J. 2002, “A review of literature on dynamic models of vapor compression equipment”, ASHRAE Report #4036-5

Jensen B.J., Skogestad S. 2007, “Optimal operation of simple refrigeration cycles – Part I: Degrees of freedom and optimality of sub-cooling”, Computers and Chemical Engineering, vol. 31, pp. 712–731

Jensen B.J., Skogestad S. 2007, “Optimal operation of simple refrigeration cycles – Part II: Selection of controlled variables”, Computers and Chemical Engineering, vol. 31, pp. 1590–1601

Karlsson F. 2007, “Capacity control of residential heat pump heating systems”, PhD dissertation, Chalmers University of Technology, Göteborg, Sweden

Lepore R., Remy M., Dumont E., Frère M. 2010, “Dynamic lumped-parameter model of a heat pump designed for performance optimization”, Proceedings of Simulation Systems in Buildings SSB2010, Liège, Belgium

Rasmussen B. 2002, “Control-oriented modeling of transcritical vapor compression Systems”, Master’s thesis, University of Illinois, Urbana-Champaign.

Rasmussen B. 2005, “Dynamic modeling and advanced control of air conditioning and refrigeration systems”, PhD dissertation, University of Illinois, Urbana-Champaign

Schurt L. 2009, “Mathematical modeling and multivariable control of vapor compression refrigeration Systems”. PhD dissertation, Federal University of Santa Catarina, Florianopolis-SC, Brazil (in Portuguese)

Wedekind G.L., Bhatt B.L., and Beck, B.T. 1978, *A system mean void fraction model for predicting various transient phenomena associated with two-phase evaporating and condensing flows.* International Journal of Multiphase flow, vol. 4, n°1, pp. 97–114.

Willatzen M., Pettit N.B.O.L., and Ploug-Sorensen L. 1998, *A general dynamic simulation model for evaporators and condensers in refrigeration. Part I: moving-boundary formulation of two-phase flows with heat exchange.* International Journal of Refrigeration, vol. 21, n°5, pp. 398–403.